Real-Time Crop Growth Stage Estimation Using Multi-modal Satellite Imagery

Abhijit Sinha
A.U.G. Signals Ltd.
Toronto, Canada
abhijit@augsignals.com

Sina Adham-Khiabani
A.U.G. Signals Ltd.
Toronto, Canada
sina@augsignals.com

Yifeng Li
A.U.G. Signals Ltd.
Toronto, Canada
yifeng@augsignals.com

George Lampropoulos
A.U.G. Signals Ltd.
Toronto, Canada
lampro@augsignals.com

Heather McNairn
Agriculture and Agri-Food Canada
Ottawa, Canada
heather.mcnairn@agr.gc.ca

Xianfeng Jiao
Agriculture and Agri-Food Canada
Ottawa, Canada
xianfeng.jiao@agr.gc.ca

***Abstract*—Real-time crop growth stage estimation is essential to facilitate improved crop management, disease mitigation, and resource planning. This paper describes a nonlinear filtering technique that combines weather and multi-modal satellite image data to estimate crop growth stages at the pixel level. This procedure is an improvement, in terms of efficiency and robustness, over a procedure previously published by the authors. Results show that the procedure computes pixel-level crop growth stages effectively and provides accurate estimates when compared with ground truth crop growth stage data.**

Keywords—crop phenology tracking, multi-satellite data fusion, nonlinear tracking, crop growth estimation, synthetic aperture radar, real time processing

I. INTRODUCTION

Real-time crop growth stage estimation (also referred to as phenological states) is required for precision agriculture, particularly for facilitating improved crop management, pest and disease mitigation, and resource planning. This is an input to crop management decisions, including irrigation, fertilization, pesticide application, irrigation management and harvesting. For example, information on growth stage, when coupled with information on soil moisture, can be used to determine field specific risks of sclerotinia infection in canola.

Differences in cultivars or soil and weather conditions imply that the timing of crop stages cannot be easily estimated, even when planting date is known. Traditional approaches to estimate crop growth stages using crop models can often achieve Root Mean Square Error (RMSE) of 4 days or less [1]. However, such models require detailed information on soil moisture, temperature, rainfall, solar radiation and windspeed as inputs. Even then, these models require calibration based on site-specific conditions' ground truth data [2]. Such restrictive constraints impede large scale use of these models. Regular and detailed survey of fields are necessary for farming operations. However, manual survey may not be possible given the associated costs, particularly considering large crop fields, for example in North America. Thus, even if you assess growth stage at the edge of the field, this may not be accurate for other areas of the field. However, a cost-effective regular monitoring can be achieved by satellite remote sensing. In this case, other than producers, crop insurers can also use crop growth stage estimates as a cost-effective alternate to manual field survey for a large area, after insurance claims.

In conventional remote sensing approaches, electro-optical sensors have been used in pair of a limited weather data e.g., temperature for post-season growth estimation. However, gaps in data coverage, due to cloud interference, limit the effectiveness of any solution solely based on visible and infrared Earth observation sensors. Hence, reliable, and frequent access to remote sensing data is desirable to determine time-specific and field-specific growth stages. This can be achieved by combining data from electro-optical sensors with synthetic aperture radar (SAR) imagery. The latter provides all-weather, day-night, large-area surveillance with high-spatial-resolution coverage. Moreover, these two data types are complementary in nature for many applications including crop growth monitoring. While optical data provides information on color and temperature of objects, SAR response largely depends on the geometrical and dielectric properties. SAR sensors are usually demonstrating meaningful sensitivity to the variations of canopy structures depending on crop type and its growth stage.

Estimation of crop phenological stages has sometimes been considered as a classification problem [3,4]. Such approach lacks in exploiting the information that growth stages change in a specific sequence. Among recursive procedures, a particle filter-based method is developed for growth stage estimation of rice [5]. This procedure uses linear combination of dual-pol TerraSAR-X parameters as state variables. Due to this selection, the procedure has limitations in terms of computational complexity and also extension of the formulation to fuse multi-satellite data, e.g., optical and SAR, is not straightforward [6].

In our previous work [6], a number of above discussed limitations are addressed by incorporating crop maturity level as a variable directly related to crop growth stages. The procedure, in [6], models response of remote sensor data to crop growth stages using gathered ground truth. Recursive estimation is performed using particle filter, which is initialized based on the variability of planting date. Crop maturity level is predicted

"This work was partially funded by the Agri-Innovation Program of Agriculture and Agri-Food Canada". Patent pending.

979-8-3503-3959-8/23/$31.00 ©2023 IEEE

based on growing degree days (GDD) data, which is computed from the average daily temperature. Crop maturity is updated based on the normalized difference between model predicted sensor response and observed sensor response. The procedure in [6] is validated for field-level canola growth stage estimation using SAR data from TerraSAR-X and RADARSAT-2.

The current work extends the field level estimates to pixel-level (10m) uses both SAR and optical data and applies the procedure to a set of crops (canola, corn, soybean, and wheat). Instead of particle filter, a grid-based approach is developed to reduce the computational cost of performing estimation over a large area without negatively effecting estimation performance. This paper also provides detailed description of the estimation process, which is not available in [6]. In this paper, Section II provides details of the developed crop growth stage estimation procedure; and Section III discusses the results. In Section IV conclusions are provided and future work is described.

II. Crop Growth Estimation Procedure

In this section, choice of state variable is discussed, optical and SAR imagery feature selection and modelling is described and steps of grid-based filtering are discussed.

A. Choice of State Variable

Choice of state variable is a key aspect of development of a recursive estimator. The ground truth crop growth stages available for this work was collected in BBCH (Biologische Bundesanstalt, Bundessortenamt and CHemical) scale which is a code system based on Zadoks scale [7]. BBCH is defined by a finite set of integer values. The discrete nature of BBCH makes it unsuitable to be used as a state variable. Also, changes in BBCH are highly non-linear with respect to calendar days or key weather indices, such as GDD. GDD is accumulated averaged daily temperature range, subtracted by the assumed minimum temperature required for growth to proceed. For most plants, phenological development is strongly related to GDD. Hence, it has been used by agronomists to predict growth stages when the planting date or date of another key growth stage is known. Due to the of GDD's characteristics, a state variable, crop maturity [6], is developed which has a linear relationship with GDD. Crop maturity is a continuous variable that maps the growth stages of each crop within [0,1]. For a crop to reach a specific BBCH, a certain number of GDD is required on average. Crop maturity for any growth marker is the ratio of average GDD required to reach that stage to the average GDD required by a crop during its lifetime (Eq. 1). This makes BBCH easily convertible to crop maturity and vice versa. GDD range required by crops to reach a specific BBCH code can be found from agronomy sources, such as North Dakota Agriculture Weather Network[1]. Instead of GDD, calendar days can also be used to compute crop maturity. However, this will make crop maturity and crop growth estimation procedures specific to a location.

$$\text{Crop maturity(n)} = \frac{\text{Avg. GDD the crop takes to reach BBCH (n) from seeding date}}{\text{Avg. GDD crop lifetime needs}} \quad (1)$$

B. Satellite Imagery Feature Selection

Many studies have reported strong dependency of growth stages with satellite vegetation indices derived from optical imagery [2] and SAR-imagery-derived polarimetric parameters [8, 9]. In this work, two types of SAR satellite data are used: C band compact polarimetric data from the RADASAT Constellation Mission (RCM) and C-band dual-pol data from Sentinel 1. In this research, the SAR data is combined with Sentinel 2 as multispectral data. For each data type, tens of features can be extracted. As the feature set corresponding to each data type is highly co-dependent, using all of the features for crop growth estimation will increase computational cost and redundancy as well as possible large biases in estimated growth stage. This necessitates the development of a robust selection procedure using ground truth data of crop maturity. As ground truth may not be available on image acquisition days, crop maturity is interpolated using GDD data. This provides crop maturity and image feature pair for each ground available satellite image acquisition date. Moreover, to address the limitations of correlation measures, in this work Maximal Information Coefficient (MIC) [10] is used which computes normalized mutual information. MIC value ranges between [0,1] with higher value representing higher dependency between variables.

Based on pairwise MIC values among all features and crop maturity, a greedy algorithm is developed for imagery feature selection. Steps of the procedure are as follows [9]:

1. Sort image features based on their MIC with crop maturity and truncate the list based on a threshold T_1
2. Initialize selected feature set S by adding the image feature with the highest MIC with crop maturity.
3. For each remaining feature
    a. Add the feature to S if its highest MIC with the features already in S is less than threshold T_2
4. If success in Step 3a, repeat Step 3.

The above procedure ensures that the selected features have high MIC with crop maturity and have low pairwise MIC among the selected set. The selection procedure is performed for each satellite image type.

The list of selected features is provided below:

- RCM: Conformity, Relative phase delta, RV, Contrast, Stokes 3
- Sentinel 1: Entropy, C22, Degree of Linear Polarization, Stokes 1
- Sentinel 2: MTCI, CVI, MSI, MYVI, B2

C. Measurement Model

Assuming satellite features as observations, and satellite image feature response model to growth stages as measurement model. The model can be developed using ground truth growth stages and image data. As an example, ground truth MTCI feature (Sentinel 2) corresponding to corn is shown against crop maturity in Fig. 1. At each point of crop maturity, the feature distribution is assumed to be Gaussian. The mean and standard deviation of this distribution are computed at regular intervals on the maturity axis. Expected feature distribution at any value of crop maturity, within the range where feature data exists, is obtained through interpolation.

1 https://ndawn.ndsu.nodak.edu/help-canola-growing-degree-days.html

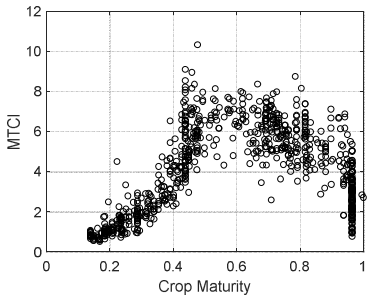

Fig. 1: Corn maturity vs. Sentinel 2 feature MTCI.

D. Crop Growth Stage Tracking Filter

Fig. 2 shows stages of the tracking filter. At initialization, the crop maturity is assigned by a value based on the variability of base GDD values of the crop under consideration at planting (or seeding). Starting point of GDD accumulation varies crop to crop. Daily prediction is performed using GDD data when images are available [6]. In this work in the contrary, if satellite image(s) are available on a particular day, crop maturity can be updated based on the statistical deviation of expected features from the measured features. Data from different satellite types are seamlessly fused in this measurement level fusion architecture. The key difference between [6] and the current work is the choice of nonlinear filter. While [6] used particle filter, in this work grid-based tracker is used to reduce computational cost and remove randomness from the estimates given specific measurements. Unlike in [6], which performs field-based crop maturity estimates, this work performs the estimation at each 10m×10m pixel.

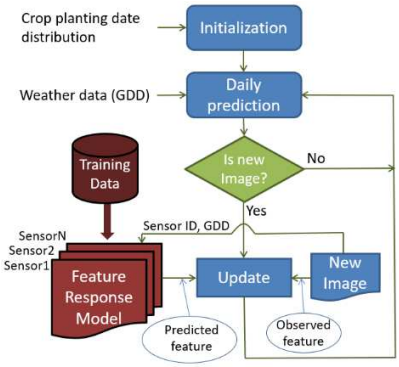

Fig. 2: Crop growth stage tracking filter.

Since the number of pixels can be very large, the growth stages statistics are approximated as Gaussian to reduce storage requirement. For a particular pixel, let $\hat{x}(i|i)$ denote the estimated state at time-step i given data up to that point and $P(i|i)$ denote the corresponding error variance.

The initialization point for each crop is set when their expected maturity exceeds a threshold. The threshold corresponds to a GDD that represents the latest planting time. Following (1), the expected maturity at the initialization point, denoted by x_0, is computed as the ratio of accumulated GDD at the initialization point to the average GDD for the crop lifetime.

Initialization is performed as follows:

$$\hat{x}(0|0) = x_0/2 \text{ and } P(0|0) = {x_0}^2/12 \quad (2)$$

The above equation assumes crop planting is uniformly distributed between the 0 GDD (at this point the crop can be planted) and $x_0 \times$ average GDD for crop lifetime. So, Daily prediction is performed from day k to day $k+1$ as follows:

$$\hat{x}(k+1|k) = \hat{x}(k|k) + \Delta x(k+1) \quad (3)$$

where $\Delta x(k+1)$ is the expected change in maturity. It is the ratio of change of GDD on $k+1$ th day to the average GDD for the crop lifetime. Prediction covariance is obtained as follows:

$$P(k+1|k) = P(k|k) + \Delta x(k+1)^2 q^2 \quad (4)$$

where q is a constant that is computed from the ground truth variation of GDD at different crop maturity values.

For update $2N+1$ samples are obtained from the Gaussian $\left(\hat{x}(k+1|k), P(k+1|k)\right)$ at uniform intervals between $\hat{x}(k+1|k) - 3.5\sqrt{P(k+1|k)}$ and $\hat{x}(k+1|k) + 3.5\sqrt{P(k+1|k)}$. Let the n th sample be denoted as $\hat{x}_n(k+1|k)$ and corresponding pdf be denoted as $p_n(k+1|k)$, which is computed as

$$p_n(k+1|k) = \frac{1}{\sqrt{2\pi P(k+1|k)}} \mathrm{e}^{-\frac{0.5}{P(k+1|k)}\left(\hat{x}_n(k+1|k) - \hat{x}(k+1|k)\right)^2} \quad (5)$$

Satellite image feature distribution assuming maturity $\hat{x}_n(k+1|k)$ being the truth is obtained from the measurement model. Let the Gaussian distribution be denoted as $\left(f_n\left(\hat{x}_n(k+1|k)\right), \Sigma_n\left(\hat{x}_n(k+1|k)\right)\right)$ and the measured feature be denoted as $f_{\text{meas}}(k+1)$. Then, a posteriori likelihood of the n-th grid point (crop maturity) is given by:

$$l_n(k+1|k+1) = p_n(k+1|k) \frac{1}{\sqrt{|2\pi\Sigma_n|}} \mathrm{e}^{-0.5(f_n - f_{\text{meas}})' {\Sigma_n}^{-1} (f_n - f_{\text{meas}})} \quad (6)$$

The updated Gaussian distribution is obtained as follows:

$$\hat{x}(k+1|k+1) = \frac{1}{c}\sum_{n=1}^{2N+1} l_n(k+1|k+1)\hat{x}_n(k+1|k) \quad (7)$$

$$P(k+1|k+1) = \frac{1}{c}\sum_{n=1}^{2N+1} l_n(k+1|k+1)\hat{x}_n(k+1|k)^2 - \hat{x}(k+1|k+1)^2 \quad (8)$$

where c is a normalization constant, given by

$$c = \sum_{n=1}^{2N+1} l_n(k+1|k+1) \quad (9)$$

III. Results

Results from the crop growth estimation procedure developed in this work are compared to the ground truth data collected at a specific location during the season of 2021 in Carmen, Manitoba (Canada). Here, we considered the starting GDD or $x_0 \times$ average GDD for crop lifetime equal to 20. Also, the total number of grid points is set to be 81, i.e. $N = 40$.

In Fig. 3 and Fig. 4 crop maturity estimates are compared to ground truth data collected weekly at specific canola and wheat pixel locations. The solid green line shows daily crop maturity estimates, and the red dash-dot and dashed lines show the upper and lower limits of 95% confidence interval. The sign '+' corresponds to ground truth crop maturities, which are converted

from BBCH values. As shown in Fig. 3 and Fig. 4 the ground truth matches well with the estimates, in most of the cases. However, there are ground truth observations that appears to have inconsistent values (Fig. 3), such as large deviation from the remaining ground truth sequence. Overall standard errors in number of days are 5.7 days for canola, 4.9 days for corn, 5.8 days for soybean and 4.9 days for wheat. In all cases, except for soybeans, the error data is averaged over twelve ground truth data locations over the 2021 season, one from each of 12 fields. For soybean, eleven ground truth locations are determined to be reliable. Note that a large part of the error standard deviations is explained by what appears to be erroneous ground truth data.

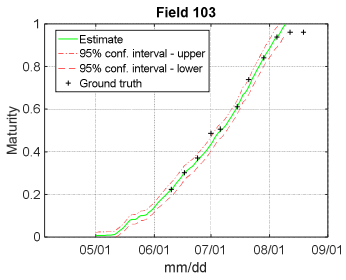

Fig. 3: Estimated and observed canola growth stages at a pixel in field 103.

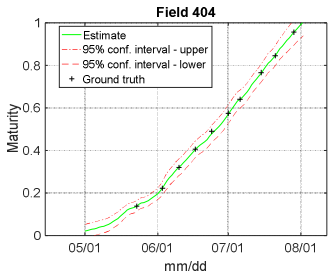

Fig. 4: Estimated and observed wheat growth stage at a pixel in field 404.

Fig. 5 shows the growth stages of canola on four different days within the 2021 season in Carman, MB. A color code used to show canola's phenology. The darker shades of any color mean an early phase of corresponding growth stage. As shown in Fig. 5, canola is at the initial stage on June 6th. On June 26th canola reaches close to flowering. For some canola fields, different parts are at different growth stages. Clear separation of such areas show that pixel level crop growth monitoring is effective. Many canola fields reach pod development on July 16th and on August 6th in most cases canola is ripe.

IV. Conclusions and Future Work

In this work, a recursive nonlinear estimator is developed that efficiently combines weather and multi-modal satellite image data to estimate crop growth stages. In terms of computational efficiency and robustness, the procedure is an upgrade from a procedure previously published by the authors. The procedure, in the current work, is applied to fuse SAR data from RCM and Sentinel 1 with optical data from Sentinel 2 to achieve improved crop growth stage estimation. Growth stages of four crops, namely canola, corn, soybean and wheat, are estimated at fields in Carman, Manitoba (Canada) for the 2021 season and results are compared to ground truth collected weekly at forty-seven fields. The standard error of the growth stage estimates, when compared to the ground truth, are below 6 days even though the collected ground truth data appears to be anomalous in some cases. Evolution of canola over the season shows that the procedure can effectively distinguish different levels of maturity of a crop at the same field.

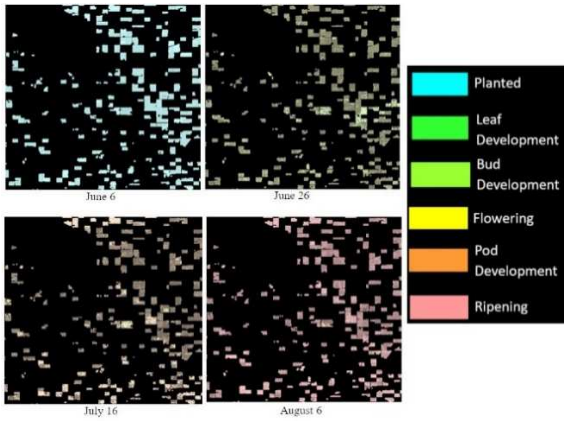

Fig. 5: Canola growth Stages in Carmen, MB on four days of 2021 season.

In the future, further analysis will be performed on the parameters used in the crop growth stage estimation procedure. For example, the number of grid points used in the update stage of the filter will be analyzed with the objective of further reducing the computational cost without effecting the growth stage estimation performance.

References

[1] H. S. Yang, A. Dobermann, J. L. Lindquist, D. T.Walters, T. J. Arkebauer, & K. G. Cassman, "Hybrid-maize—A maize simulation model that combines two crop modeling approaches," Field Crops Research, 87(2–3), pp. 131–154, 2004.

[2] L. Zeng, B. D. Wardlow, R. Wang, J. Shan, T. Tadesse, M. J. Hayes, D. Li, "A hybrid approach for detecting corn and soybean phenology with time-series MODIS data," Remote Sensing of Environment, Vol. 181, pp. 237-250, 2016.

[3] A. Mercier et al. "Evaluation of Sentinel-1 & 2 time series for predicting wheat and rapeseed phenological stages." ISPRS Journal of Photogrammetry and Remote Sensing 163, pp 231-256, 2020.

[4] H. Wang, et al. "Crop phenology retrieval via polarimetric SAR decomposition and Random Forest algorithm." Remote Sensing of Environment 231, pp. 111234,.2019.

[5] C. G. De Bernardis, F. Vicente-Guijalba, T. Martinez-Marin, J. M. Lopez-Sanchez, "Estimation of key dates and stages in rice crops using dual-polarization SAR time series and a particle filtering approach," IEEE J. Sel. Top. Appl. Earth Observ. Remote Sens. 8 (3), 1008–1018, 2015.

[6] H. McNairn, X. Jiao, A. Pacheco, A. Sinha, W. Tan, and Y. Li, "Estimating canola phenology using synthetic aperture radar," Remote Sensing of Environment (ELSEVIER), Volume 219, Pages 196-205, December 2018.

[7] U. Meier, et al. "The BBCH system to coding the phenological growth stages of plants–history and publications." Journal für Kulturpflanzen 61.2: 41-52, 2009.

[8] F. Canisius, et al, "Tracking crop phenological development using multi-temporal polarimetric Radarsat-2 data," Remote Sens. Environ. Vol. 210, pp. 508–518, 2017.

[9] A. Sinha, W.Tan, Y. Li, H. McNairn, X. Jiaob, M. Hosseini, "Applying a particle filtering technique for canola crop growth stage estimation in Canada," SPIE Remote Sensing Conf., Sept. 2017.

[10] D. Reshef, et al, "Detecting novel associations in large datasets," Science, Vol. 334, Issue 6062, pp. 1518-1524, 2011.